



Title	Big bang nucleosynthesis constraints on varying electron mass solution to the Hubble tension
Author(s)	Seto, Osamu; Toda, Yo
Citation	Physical Review D, 107(8), 83512 https://doi.org/10.1103/PhysRevD.107.083512
Issue Date	2023
Doc URL	http://hdl.handle.net/2115/90072
Rights	©2023 American Physical Society
Type	article
File Information	PhysRevD.107.083512.pdf



[Instructions for use](#)

Big bang nucleosynthesis constraints on varying electron mass solution to the Hubble tension

Osamu Seto^{*} and Yo Toda[†]*Department of Physics, Hokkaido University, Sapporo 060-0810, Japan*

(Received 4 July 2022; accepted 21 March 2023; published 13 April 2023)

A cosmological model with a time-varying mass of electrons seems a promising solution for the so-called Hubble tension. We examine the big bang nucleosynthesis (BBN) constraints on the time-varying electron mass model because a larger electron mass gives rise to the smaller weak interaction rate for the proton and neutron conversion, which could affect the light element abundance. Additionally, different inferred cosmological parameters, primarily baryon asymmetry, keeping the cosmic microwave background power spectrum unchanged could affect the abundance of light element. We find that the resultant proton-to-neutron ratio is not so much sensitive with respect to the electron mass because the change of weak interaction rate becomes important after the cosmic temperature becomes lower than the electron mass, while the slightly smaller present Hubble parameter and the electron mass are indicated if the BBN data are taken into account. We also find that the baryon density is more stringently constrained by the baryon acoustic oscillation data rather than the BBN. We have derived the ratio of the electron mass at early Universe and the present $m_e/m_{e0} = 1.0028 \pm 0.0064$ and $H_0 = 68.0 \pm 1.1$ km/s/Mpc.

DOI: [10.1103/PhysRevD.107.083512](https://doi.org/10.1103/PhysRevD.107.083512)

I. INTRODUCTION

The cosmic expansion is one of the most fundamental properties of our Universe. The present expansion rate called the Hubble constant H_0 has been measured by various methods. The direct measurements of H_0 with low redshifts distant ladders report larger values of H_0 than the cosmological estimation $H_0 = 67.4 \pm 0.5$ km/s/Mpc with the temperature and polarization anisotropy of the cosmic microwave background (CMB) by Planck (2018) [1]. The SH0ES collaboration reported $H_0 = 73.04 \pm 1.04$ km/s/Mpc by using Cepheids and type Ia supernovae as the standard candle in Ref. [2]. Another local measurement using the Tip of the Red Giant Branch as distance ladders [3] and the H0LiCOW collaboration by the measurements of lensed quasars [4] also report a larger value of H_0 than the Planck results. The discrepancy between various low-redshift measurements of the Hubble constant and the value inferred from the CMB temperature anisotropy by Planck (2018) is now regarded as the Hubble tension or the H_0 tension.

This problem has been the object of many attempts [5,6]. One of the simplest approaches is to introduce additional relativistic degrees of freedom parametrized by $\Delta N_{\text{eff}} = N_{\text{eff}} - N_{\text{eff}}^{\text{SM}}$, where N_{eff} is the total effective relativistic degrees of freedom and $N_{\text{eff}}^{\text{SM}}$ is its predicted value by the standard model (SM) of particle physics [7–10]. The measured angular size $\theta_* \equiv r_{s*}/D_{M*}$ of the acoustic scale

of the CMB infers a shorter angular diameter distance $D_{M*} \propto 1/H_0$, if the sound horizon scale r_{s*} at the recombination epoch is shorter by the extra energy density with a larger N_{eff} . The preferred value has been suggested as $0.2 \lesssim \Delta N_{\text{eff}} \lesssim 0.5$ based on the CMB, the baryon acoustic oscillation (BAO) and the SH0ES in Ref. [1]. If we also account for the successful big bang nucleosynthesis (BBN) in the analysis, a smaller value as $0.2 \lesssim \Delta N_{\text{eff}} \lesssim 0.4$ is preferred [11] because the extra energy density could speed up the cosmic expansion at the BBN epoch and alter the resultant Helium mass fraction Y_p . Such additional energy density is limited not only by the BBN but by the CMB itself as well. If the cosmic expansion rate at the recombination time is increased by extra energy densities to reduce the sound horizon scale, then simultaneously the relative scale between the sound horizon and the photon diffusion (Silk damping) length is also changed. As a result, all models of this class are confronted with the limitation [12].

A cosmological model with a time-varying electron mass m_e [13,14] can effectively reduce the sound horizon scale [15–18]. As the energy level of hydrogen $E^{\text{H}} \propto m_e$ and the Thomson scattering cross section $\sigma_T \propto 1/m_e^2$, the time-varying electron mass could reduce both the sound horizon scale and the Silk damping scale, which does not affect the power spectrum of the CMB temperature anisotropy.

In this paper, we examine other possible consequences of the time-varying electron mass model in which the mass of the electron has been about a few percent larger than the present value before the recombination. Such one important

^{*}seto@particle.sci.hokudai.ac.jp[†]y-toda@particle.sci.hokudai.ac.jp

event in the early Universe is the BBN where light elements were synthesized. The helium mass fraction has been reported as $Y_p = 0.2449 \pm 0.0040$ from the recent observation data [19]. The deuterium abundance D/H has been measured as $(D/H) = (2.527 \pm 0.030) \times 10^{-5}$ [20]. However, if the electron mass is larger than the present value, then the abundance of synthesized light elements would be altered [21–25]. One reason is that the decay rate of the neutron n to the proton p^+ , electron e^- and neutrino ν also depends on the electron mass as [26]

$$\Gamma(n \rightarrow p^+ e^- \nu) = \frac{G_F^2}{2\pi^3} (1 + 3g_A^2) m_e^5 \lambda_0(q), \quad (1)$$

$$\lambda_0(q) = \int_1^q dx x(x-q)^2 (x^2-1)^{1/2}, \quad (2)$$

with $q = Q/m_e$, where G_F is the Fermi constant, g_A is the axial-vector coupling of the nucleon, and $Q = m_n - m_p$ is the difference between the proton mass m_p and the neutron mass m_n . The rate of weak interactions such as $\nu + n \leftrightarrow p^+ + e^-$ also depends on the electron mass [27]. Thus, it causes earlier (later) decoupling of $n \leftrightarrow p$ interactions for a larger (smaller) electron mass and results the change of the neutron to proton ratio. The prediction of the BBN is sensitive to the variation of the neutron decay rate and the weak interaction rate [28,29]. We derive the constraints on the variation of the electron mass in the early Universe, assuming that the electron mass at the BBN time is the same as at the recombination epoch and that the other fundamental parameters, such as the fine structure constant and the Fermi constant, are not varied.

II. DATA AND ANALYSIS

We conduct a Markov-chain Monte Carlo analysis on the time-varying electron mass model. We use the public Markov-chain Monte Carlo code CosmoMC-planck2018 [30]. The change of the electron mass is implemented in the neutron decay rate in the BBN era as

$$\Gamma(n \rightarrow p^+ e^- \nu_e)_{\text{BBN}} = \Gamma_{n0} \left(\frac{m_e}{m_{e0}} \right)^5 \frac{\lambda_0(Q/m_e)}{\lambda_0(Q/m_{e0})}, \quad (3)$$

through Eq. (1) with the present values of the neutron lifetime $\tau_{n0} = 1/\Gamma_{n0} = 879.4$ second as well as in the $n \rightarrow p^+$ weak interaction rate through its phase space integral [27]

$$\lambda(n \rightarrow p^+) \propto \left(\int_{-\infty}^{-m_e-Q} \frac{x^2(Q+x)^2 \sqrt{1 - \frac{m_e^2}{(Q+x)^2}}}{(e^{\frac{x}{T_\nu}} + 1)(e^{-\frac{Q+x}{T}} + 1)} dx + \int_{m_e-Q}^{\infty} \frac{x^2(Q+x)^2 \sqrt{1 - \frac{m_e^2}{(Q+x)^2}}}{(e^{\frac{x}{T_\nu}} + 1)(e^{-\frac{Q+x}{T}} + 1)} dx \right), \quad (4)$$

with T_ν being the temperature of neutrinos and similar in the $p^+ \rightarrow n$ weak interaction rate. From now on, m_e denotes the electron mass in the early Universe and we use the present electron mass $m_{e0} = 511$ keV [31].

We analyze the models by referring to the following cosmological observation datasets. We include both temperature and polarization likelihoods for high l PLIK ($l = 30$ to 2508 in TT and $l = 30$ to 1997 in EE and TE) and low l COMMANDER and low E SimAll ($l = 2$ to 29) of Planck (2018) measurement of the CMB temperature anisotropy [1]. We also include Planck lensing [32] and data of the BAO from 6dF [33], DR7 [34], and DR12 [35]. We use the datasets of the Y_p [19] and D/H measurements [20] to impose the BBN constraints.

III. RESULT AND DISCUSSION

We calculate light elements abundance by using PArthENoPE3.0-Standard [36] with the above modification. The change of phase space in Eq. (4) by varying the electron mass induces the enhancement or suppression of the $p^+ \leftrightarrow n$ interaction rate. We show that the value of $\lambda(n \rightarrow p^+)$ for $m_e = 1.03 \times m_{e0}$ is normalized by that for m_{e0} in Fig. 1. As can be seen in Fig. 1, the interaction rate is insensitive with respect to m_e at a high temperature $T \gg m_e \sim m_{e0}$, while the interaction rate changes at a low temperature $T \ll m_e \sim m_{e0}$, where it is dominated by the beta decay of neutron $n \rightarrow p^+ e^- \bar{\nu}$ with the decay rate given by Eq. (1). Indeed, for the case shown in Fig. 1, the neutron decay rate is reduced by about 4.6% due to the increasing of the electron mass $m_e = 1.03 \times m_{e0}$. We notice that the effect on the $p^+ \leftrightarrow n$ reaction rate by different electron mass appears only after

$$T \lesssim m_{e0}. \quad (5)$$

The neutron-to-proton ratio

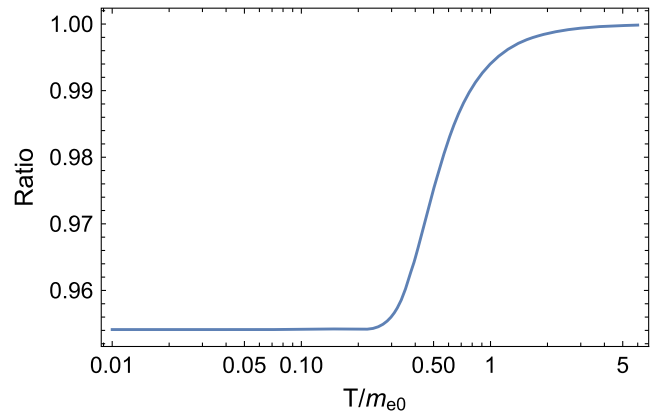


FIG. 1. The suppression of $\lambda(n \rightarrow p^+)$ for $m_e = 1.03 \times m_{e0}$ as a function of T/m_{e0} .

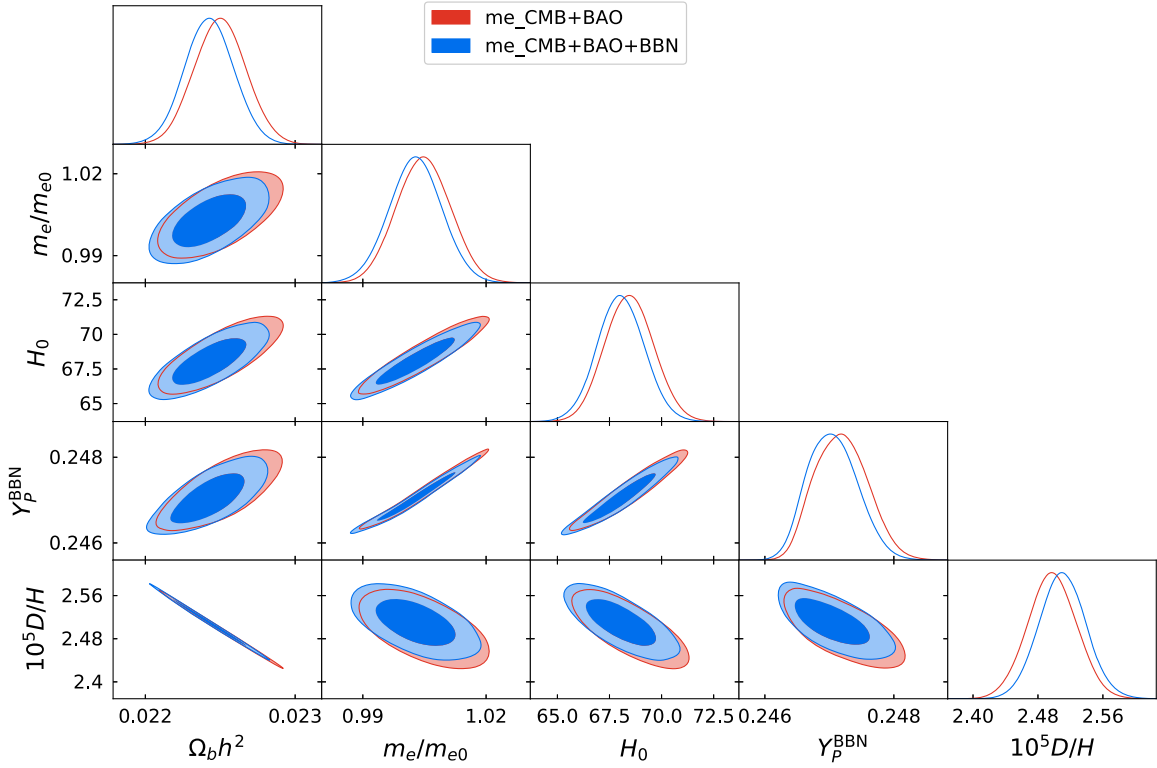


FIG. 2. Posterior distributions of light elements abundance Y_p and D/H , m_e/m_{e0} , and H_0 for several values of m_e/m_{e0} .

$$\frac{n}{p} \simeq \exp\left(-\frac{Q}{T_D}\right) \simeq \frac{1}{6} \quad (6)$$

is realized with the decoupling temperature of $p^+ \leftrightarrow n$ interaction, $T_D \simeq 0.8$ MeV [37]. By comparing with Eq. (5), we find that the effect of varying electron mass just starts to appear and is not yet so significant when the $p^+ \leftrightarrow n$ conversion freezes out at $T \simeq T_D$.

So far, we have found that the resultant proton-to-neutron ratio is not affected much for a fixed baryon-to-photon ratio η . The time-varying electron mass model looks an effective solution to the Hubble tension because the electron mass variation effect on the CMB power spectrum can be absorbed by varying the inferred baryon density parameter $\Omega_b h^2$ and the matter density parameter $\Omega_m h^2$ due to the parameter degeneracy [17]. The other way to affect light elements abundance by the variation of the electron mass is through the change of the inferred baryon asymmetry $\Omega_b h^2$. As is well known, the D/H would reduce as the inferred baryon asymmetry $\Omega_b h^2$ becomes larger.

This can be seen in the 2D posterior distributions of cosmological and BBN parameters of Fig. 2. We do not find the significant difference for varying electron mass model by including BBN data because the p/n ratio and the resultant helium fraction are not affect much by the variation of the electron mass, as has been discussed. Since the $\Omega_b h^2$ in time-varying electron mass models has been

adjusted to fit the CMB spectrum, for the same inferred somewhat smaller $\Omega_b h^2$, a larger D/H is indicated.

To see the detail of χ^2 , the predicted H_0 , Ω_m , Y_p , and D/H of the best fit point in the varying m_e model and the Λ cold dark matter (Λ CDM) model are listed in Table I for the dataset of CMB, BAO, and BBN. We find, between the constraints on the varying m_e model, that the BAO constraint is more stringent than the BBN. We also show the prior dataset dependence in Table II.

TABLE I. The best-fit χ^2 of the varying m_e model for other cosmological models and its comparison to the Λ CDM model. Here, we take $N_{\text{eff}}^{\text{SM}} = 3.046$ [7] of the default value in the CAMB.

Model	Varying m_e	Λ CDM
$\Omega_b h^2$	0.0228808	0.0226626
m_e/m_{e0}	1.01705	1
H_0	71.2286	68.4235
Ω_m	0.286295	0.301459
Y_p^{BBN}	0.248037	0.246972
$10^5 D/H$	2.4326	2.46674
χ_{Cooke}^2	3.89684	2.59375
χ_{Aver}^2	0.613477	0.267478
χ_{CMB}^2	2776.91	2777.93
$\chi_{H_0}^2$	3.96685	21.9865
χ_{BAO}^2	9.95825	5.37674
χ_{prior}^2	3.49538	4.57984
χ_{total}^2	2798.84	2812.73

TABLE II. 68% limits for various datasets.

Dataset	CMB + BAO	CMB + BAO + BBN	CMB + BAO + BBN + R21
$\Omega_b h^2$	0.02250 ± 0.00017	0.02243 ± 0.00016	0.02273 ± 0.00014
m_e/m_{e0}	1.0048 ± 0.0065	1.0028 ± 0.0064	1.0182 ± 0.0048
H_0	68.5 ± 1.2	68.0 ± 1.1	70.99 ± 0.79
Y_P^{BBN}	$0.24719^{+0.00038}_{-0.00045}$	$0.24705^{+0.00035}_{-0.00043}$	0.24804 ± 0.00030
$10^5 D/H$	2.498 ± 0.030	2.510 ± 0.029	2.458 ± 0.024

IV. SUMMARY

We have investigated the BBN constraints on a time-variable electron mass model as a solution to the Hubble tension. There are two ways that the BBN prediction can be influenced. One is caused by the modification of the $p^+ \leftrightarrow n$ weak interaction rate by the dependence of the electron mass, which turns out not to be significant. The other is due to the variation of $\Omega_b h^2$, because inferred cosmological parameters including $\Omega_b h^2$ are different from those in the Λ CDM to keep the CMB power spectrum unchanged for a

shorter sound horizon scale at the recombination. The inferred smaller $\Omega_b h^2$ suppresses D/H . Nevertheless, the BAO constrains the cosmological parameter more significantly than the BBN does, as shown in Table I.

ACKNOWLEDGMENTS

This work is supported in part by the Japan Society for the Promotion of Science (JSPS) KAKENHI Grants No. 19K03860, No. 19K03865, and No. 21H00060 (O. S.) and JST SPRING, Grant No. JPMJSP2119 (Y. T.).

-
- [1] N. Aghanim *et al.* (Planck Collaboration), *Astron. Astrophys.* **641**, A6 (2020); **652**, C4(E) (2021).
 - [2] A. G. Riess, W. Yuan, L. M. Macri, D. Scolnic, D. Brout, S. Casertano, D. O. Jones, Y. Murakami, L. Breuval, T. G. Brink *et al.*, *Astrophys. J. Lett.* **934**, L7 (2022).
 - [3] W. L. Freedman, B. F. Madore, D. Hatt, T. J. Hoyt, I. S. Jang, R. L. Beaton, C. R. Burns, M. G. Lee, A. J. Monson, J. R. Neeley *et al.*, *Astrophys. J.* **882**, 34 (2019).
 - [4] K. C. Wong, S. H. Suyu, G. C. F. Chen, C. E. Rusu, M. Millon, D. Sluse, V. Bonvin, C. D. Fassnacht, S. Taubenberger, M. W. Auger *et al.*, *Mon. Not. R. Astron. Soc.* **498**, 1420 (2020).
 - [5] E. Di Valentino, O. Mena, S. Pan, L. Visinelli, W. Yang, A. Melchiorri, D. F. Mota, A. G. Riess, and J. Silk, *Classical Quantum Gravity* **38**, 153001 (2021).
 - [6] E. Abdalla, G. Franco Abellán, A. Aboubrahim, A. Agnello, O. Akarsu, Y. Akrami, G. Alestas, D. Aloni, L. Amendola, L. A. Anchordoqui *et al.*, *J. High Energy Astrophys.* **34**, 49 (2022).
 - [7] G. Mangano, G. Miele, S. Pastor, T. Pinto, O. Pisanti, and P. D. Serpico, *Nucl. Phys.* **B729**, 221 (2005).
 - [8] M. Escudero Abenza, *J. Cosmol. Astropart. Phys.* **05** (2020) 048.
 - [9] K. Akita and M. Yamaguchi, *J. Cosmol. Astropart. Phys.* **08** (2020) 012.
 - [10] J. J. Bennett, G. Buldgen, P. F. De Salas, M. Drewes, S. Gariazzo, S. Pastor, and Y. Y. Y. Wong, *J. Cosmol. Astropart. Phys.* **04** (2021) 073.
 - [11] O. Seto and Y. Toda, *Phys. Rev. D* **103**, 123501 (2021).
 - [12] L. Knox and M. Millea, *Phys. Rev. D* **101**, 043533 (2020).
 - [13] J. D. Barrow and J. Magueijo, *Phys. Rev. D* **72**, 043521 (2005).
 - [14] J. D. Barrow, *Phys. Rev. D* **71**, 083520 (2005).
 - [15] P. A. R. Ade *et al.* (Planck Collaboration), *Astron. Astrophys.* **580**, A22 (2015).
 - [16] L. Hart and J. Chluba, *Mon. Not. R. Astron. Soc.* **493**, 3255 (2020).
 - [17] T. Sekiguchi and T. Takahashi, *Phys. Rev. D* **103**, 083507 (2021).
 - [18] R. Solomon, G. Agarwal, and D. Stojkovic, *Phys. Rev. D* **105**, 103536 (2022).
 - [19] E. Aver, K. A. Olive, and E. D. Skillman, *J. Cosmol. Astropart. Phys.* **07** (2015) 011.
 - [20] R. J. Cooke, M. Pettini, and C. C. Steidel, *Astrophys. J.* **855**, 102 (2018).
 - [21] J. Yoo and R. J. Scherrer, *Phys. Rev. D* **67**, 043517 (2003).
 - [22] K. Ichikawa, T. Kanzaki, and M. Kawasaki, *Phys. Rev. D* **74**, 023515 (2006).
 - [23] C. G. Scoccola, M. E. Mosquera, S. J. Landau, and H. Vucetich, *Astrophys. J.* **681**, 737 (2008).
 - [24] S. J. Landau, M. E. Mosquera, C. G. Scoccola, and H. Vucetich, *Phys. Rev. D* **78**, 083527 (2008).
 - [25] K. Hoshiya and Y. Toda, *Phys. Rev. D* **107**, 043505 (2023).
 - [26] D. A. Dicus, E. W. Kolb, A. M. Gleeson, E. C. G. Sudarshan, V. L. Teplitz, and M. S. Turner, *Phys. Rev. D* **26**, 2694 (1982).
 - [27] S. Weinberg, *Gravitation and Cosmology: Principles and Applications of the General Theory of Relativity* (John Wiley and Sons, New York, 1972).
 - [28] F. Iocco, G. Mangano, G. Miele, O. Pisanti, and P. D. Serpico, *Phys. Rep.* **472**, 1 (2009).
 - [29] R. H. Cyburt, B. D. Fields, K. A. Olive, and T. H. Yeh, *Rev. Mod. Phys.* **88**, 015004 (2016).

- [30] A. Lewis and S. Bridle, *Phys. Rev. D* **66**, 103511 (2002).
- [31] R. L. Workman *et al.* (Particle Data Group), *Prog. Theor. Exp. Phys.* **2022**, 083C01 (2022).
- [32] N. Aghanim *et al.* (Planck Collaboration), *Astron. Astrophys.* **641**, A8 (2020).
- [33] F. Beutler, C. Blake, M. Colless, D. H. Jones, L. Staveley-Smith, L. Campbell, Q. Parker, W. Saunders, and F. Watson, *Mon. Not. R. Astron. Soc.* **416**, 3017 (2011).
- [34] A. J. Ross, L. Samushia, C. Howlett, W. J. Percival, A. Burden, and M. Manera, *Mon. Not. R. Astron. Soc.* **449**, 835 (2015).
- [35] S. Alam *et al.* (BOSS Collaboration), *Mon. Not. R. Astron. Soc.* **470**, 2617 (2017).
- [36] S. Gariazzo, P. F. de Salas, O. Pisanti, and R. Consiglio, *Comput. Phys. Commun.* **271**, 108205 (2022).
- [37] E. W. Kolb and M. S. Turner, *Front. Phys.* **69**, 1 (1990).